

Fuzzy-Swarm Controller for Speed-Governor of Synchronous Generator

Dr. Abdulrahim Thiab Humod

Electrical and Electronic Engineering Department, University of Technology/Baghdad

Wisam Najm Al-Din Abed

Electrical and Electronic Engineering Department, University of Technology/Baghdad

Email:wisam_alobaidee@yahoo.com.

Received on: 2/10/2011 & Accepted on: 8/11/2012

ABSTRACT

The main objective of this work is to propose an intelligent controller to enhance the performance of hydraulic turbine speed-governor of a Synchronous Generator (SG) during different loading conditions.

The proposed mathematical model of the SG is connected to different loads in two ways. First, each load is connected individually and second, the SG loads change during the operation to ensure the robustness of controller for wide load variations.

Two types of controllers are used. The first controller is the Proportional-Integral (PI) based on Particle Swarm Optimization (PSO) technique to obtain optimal gains. The second controller is Fuzzy PD+I with gains and Membership Functions (MFs) tuned by PSO technique.

The results show the improvement of PI-PSO performance on conventional PI controller; also show the improvement in the performance of Fuzzy PD+I using PSO technique on PI-PSO.

Keywords: Synchronous Generator (S.G.), speed-governor, PI controller, fuzzy PD+I controller and Particle Swarm Optimization (PSO).

مسيطر الحشد الضبابي لحاكم سرعة المولد التزامني

الخلاصة

الهدف الاساسي من هذا العمل هو اقتراح مسيطر ذكي لتحسين اداء حاكم سرعة التوربين الهيدروليكي (**speed-governor**) للمولد المتزامن (**SG**) اثناء ظروف التحميل المختلفة. تم ربط النموذج الرياضي المقترح للمولد المتزامن مع احمال مختلفة بطريقتين. تم في الطريقة الاولى ربط كل حمل بصورة منفردة اما في الطريقة الثانية فإن الاحمال المربوطة للمولد المتزامن تتغير اثناء عمل المولد وذلك لضمان متانة المسيطر لمدى واسع من تغيير الاحمال. تم استخدام نوعان من المسيطرات. المسيطر الاول هو تناسبى-تكاملى (PI) و المعتمد على تقنية افضلية الحشد الجزئى (PSO) للحصول على قيم مثلى لربح (gains) المسيطر. والمسيطر الثانى هو من نوع (Fuzzy PD+I) مع ربح (gains) ودوال عضوية (MFs)

ضبطت بواسطة تقنية افضلية الحشد الجزيئي. وقد اظهرت النتائج تحسين اداء مسيطر PI-PSO على مسيطر PI التقليدي, و اظهرت ايضا تحسن اداء مسيطر Fuzzy PD+I والمعتمد على تقنية افضلية الحشد الجزيئي على مسيطر PI-PSO.

INTRODUCTION

Synchronous Generators (SG) are responsible for the bulk of the electrical power generated in the world today. They are mainly used in power stations and are predominantly driven either by steam or hydraulic turbines.

The study of synchronous generator control systems can roughly be divided into two parts: voltage regulation and speed-governor as shown in Figure (1). Both control elements contribute to the stability of the machine in the presence of perturbations [1].

Changes in real power affect mainly the system frequency while reactive power is less sensitive to changes in frequency and is mainly dependent on changes in voltage magnitude. Thus, real and reactive powers are controlled separately [2, 3].

In power system, both active and reactive power demands are never steady. They continuously change with the rising or falling trend [2], so satisfactory Alternating Current (AC) power system operation is obtained when frequency and voltage remain nearly constant or vary in a limited and controlled manner when active and reactive loads vary [4].

Since the voltage profile is consistently varied by load fluctuations so Automatic Voltage Regulator (AVR) is used to control the terminal voltage of SG, while the speed-governing system is used to regulate the turbine-generator speed and hence the frequency and the active power in response to load variation [5].

Whenever the real power demand changes, a frequency change occurs. This frequency error is amplified, mixed and changed to a command signal which is sent to turbine governor. The governor operates to restore the balance between the input and output by changing the turbine output [2, 3].

The speed-governor controller may be implemented in various ways from Proportional-Integral (PI), Proportional-Integral-Derivative (PID) to variable structure, Fuzzy Logic (FL), Artificial Neural Networks (ANNs) [4].

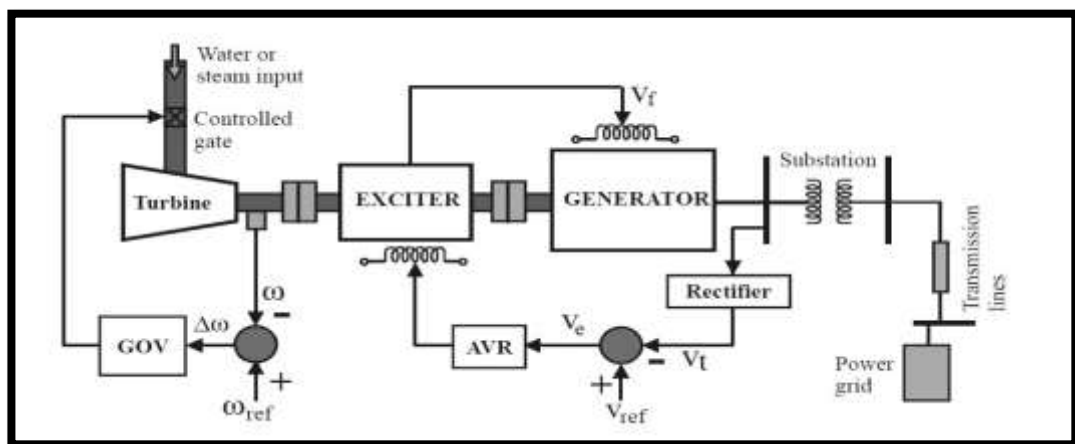


Figure (1) schematic diagram of speed-governor and AVR loop of SG [6].

MATHEMATICAL MODEL OF THE SYNCHRONOUS GENERATOR

In the late 1920s Park [7] formulated a change of variables which replaced the variables (voltages, currents and flux linkages) associated with the stator windings of a synchronous machine with variables associated with windings rotating with the rotor. In other words, transformation of the stator variables to a frame of reference in the rotor was done. Park’s transformation, which revolutionized electric machine analysis, has the unique property of eliminating all time-varying inductance from the voltage equations of the synchronous machine which occur due to:

- Electric circuits in relative motion.
- Electric circuits with varying magnetic reluctance [8].

In the basic two pole representation of a synchronous machine, the axis of the north-pole is called the direct or d-axis. The quadrature, or q-axis, is defined in the direction 90 electrical degrees ahead of the direct axis.

The mathematical model of synchronous generator with only one field winding in the d-axis and a pair of damper winding in the d- and q- axis is determined by the following equations of the winding flux linkages are as follows [9]:-

$$\Psi_q = \omega_b \int \left\{ V_q - \frac{\omega_r}{\omega_b} \Psi_d + \frac{r_s}{x_{ls}} (\Psi_{mq} - \Psi_q) \right\} . dt \quad \dots(1)$$

$$\Psi_d = \omega_b \int \left\{ V_d + \frac{\omega_r}{\omega_b} \Psi_q + \frac{r_s}{x_{ls}} (\Psi_{md} - \Psi_d) \right\} . dt \quad \dots(2)$$

$$\Psi'_{kq} = \frac{\omega_b * r'_{kq}}{x'_{lkq}} \int \left\{ (\Psi_{mq} - \Psi'_{kq}) \right\} . dt \quad \dots(3)$$

$$\Psi'_{kd} = \frac{\omega_b * r'_{kd}}{x'_{lkd}} \int \left\{ (\Psi_{md} - \Psi'_{kd}) \right\} . dt \quad \dots(4)$$

$$\Psi'_f = \frac{\omega_b * r'_f}{x_{md}} \int \left\{ E_f + \frac{x_{md}}{x'_{lf}} (\Psi_{md} - \Psi'_f) \right\} . dt \quad \dots(5)$$

$$\Psi_{mq} = XMQ \left(\frac{\Psi_q}{x_{ls}} + \frac{\Psi'_{kq}}{x'_{lkq}} \right) \quad \dots(6)$$

$$\Psi_{md} = XMD \left(\frac{\Psi_d}{x_{ls}} + \frac{\Psi'_{kd}}{x'_{lkd}} + \frac{\Psi'_f}{x'_{lf}} \right) \quad \dots(7)$$

Where, $\frac{1}{xMQ} = \frac{1}{x_{mq}} + \frac{1}{x'_{lkq}} + \frac{1}{x_{ls}}$ & $\frac{1}{xMD} = \frac{1}{x_{md}} + \frac{1}{x'_{lkd}} + \frac{1}{x'_{lf}} + \frac{1}{x_{ls}}$

The subscripts, d and q refer to the quantities on the direct and quadrature axis respectively, md and mq refer to magnetizing on direct and quadrature axis respectively, kd and kq refer to damper winding on direct and quadrature axis respectively and f refer to field on direct axis, Ψ refer to flux linkage in (Wb.turns/s v), ω_b refer to base electrical angular frequency in (rad/second), ω_r refer to rotor speed in (rad/second), r_s refer to stator winding resistance in(Ω), x_{ls} refer to stator winding leakage reactance in (Ω), x'_{lf} refer to d-axis field winding leakage reactance in (Ω) and E_f refer to steady state field excitation voltage in (V).

Having the values of the flux linkages of the windings and those of the mutual flux linkages along the d- and q- axis , we can determine the winding currents using [9]:-

$$i_q = \frac{\Psi_q - \Psi_{mq}}{x_{ls}} \quad \dots(8)$$

$$i_d = \frac{\Psi_d - \Psi_{md}}{x_{ls}} \quad \dots(9)$$

$$i'_{kd} = \frac{\Psi'_{kd} - \Psi_{md}}{x'_{lkd}} \quad \dots(10)$$

$$i'_{kq} = \frac{\Psi'_{kq} - \Psi_{mq}}{x'_{lkq}} \quad \dots(11)$$

$$i'_f = \frac{\Psi'_f - \Psi_{md}}{x'_{lf}} \quad \dots(12)$$

The electromechanical torque developed by a machine with p-pole in generating conversion is:

$$T_{em} = \frac{3}{2} \frac{P}{2 * \omega_b} (\Psi_d i_q - \Psi_q i_d) \quad \dots(13)$$

Where p=number of poles, and T_{em} is the electromechanical torque in (N.m).

The net acceleration torque can expressed by :

$$T_{em(pu)} + T_{mech(pu)} - T_{damp(pu)} = 2M \cdot \frac{d(\frac{\omega_r}{\omega_b})}{dt} = 2M \cdot \frac{d[\frac{\omega_r - \omega_e}{\omega_b}]}{dt} \quad \dots(14)$$

Where M is the inertia coefficient in second, $T_{mech(pu)}$ is the externally applied mechanical torque in the direction of rotation in per unit, and $T_{damp(pu)}$ is the frictional torque in per unit.

The simulink program of mathematical model of the synchronous generator is represented in Figure (2), the details of q-circuit, d-circuit and rotor circuit of Figure (2) are shown in Appendix (A).

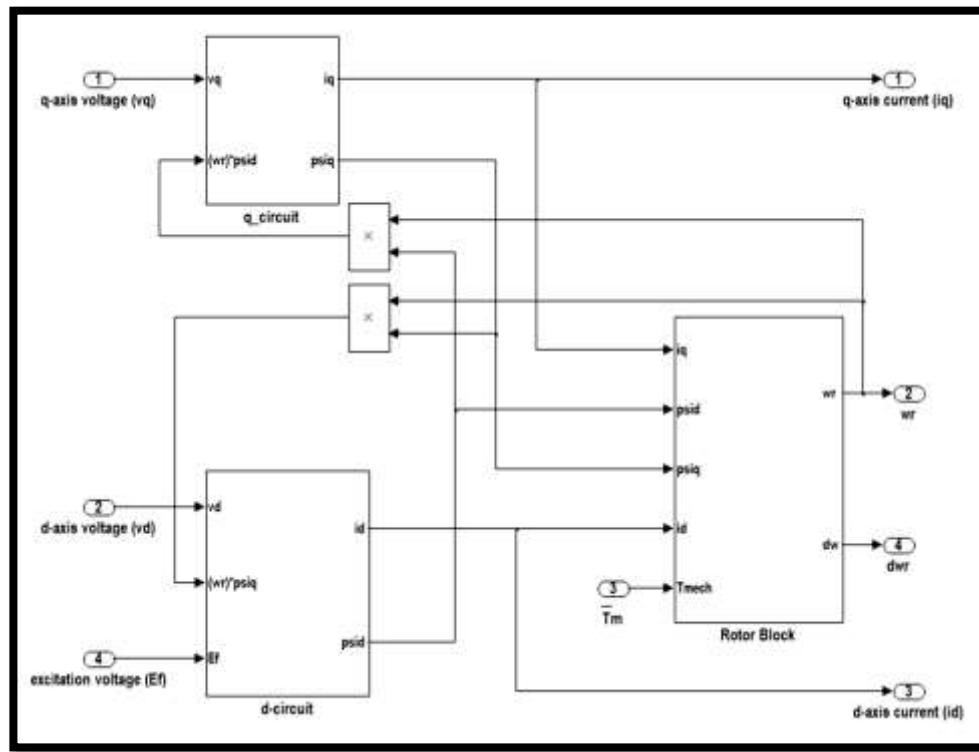


Figure (2) Simulink program of S.G.

PRIME MOVERS

Electric generators convert mechanical energy into electrical energy. The mechanical energy is produced by prime movers. Prime movers are mechanical machines convert primary energy of a fuel or fluid into mechanical energy. They are also called turbines or engines. The fossil fuels commonly used in prime movers are coal, gas, oil, or nuclear fuel [4].

Hydraulic turbines derive power from the force exerted by water as it falls from an upper to a lower reservoir. The vertical distance between the upper reservoir and the level of the turbine is called the head [5, 10].

NONLINEAR TURBINE MODEL [11]

When, the hydraulic turbine representation in system stability studies was largely based on the linear model transfer function. However, such a model is inadequate for studies involving large variations in power output and frequency. In this section, a description of nonlinear model was introduced, which is more appropriate for large-signal time-domain simulations.

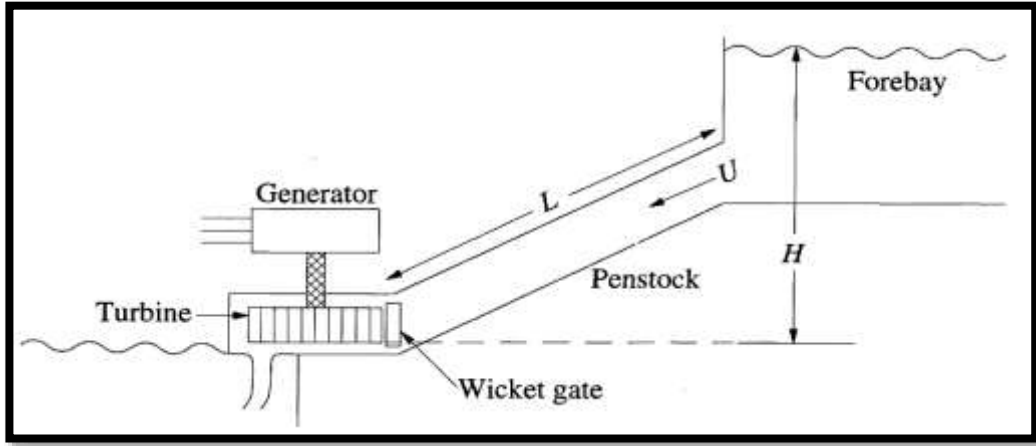


Figure (3) Schematic of a hydroelectric plant.

The basic hydrodynamic equations of hydraulic turbine are [11]:

$$\bar{H} = \left(\frac{\bar{U}}{\bar{G}}\right)^2 \quad \dots (15)$$

$$\frac{\bar{U}}{\bar{H} - \bar{H}_0} = \frac{-1}{T_w S} \quad \dots (16)$$

$$\bar{P}_m = (\bar{U} - \bar{U}_{NL}) \bar{H} \quad \dots(17)$$

Where:

\bar{H} = hydraulic head at gate in per unit.

\bar{U} = water velocity in per unit.

\bar{G} = ideal gate opening in per unit.

\bar{H}_0 = initial steady-state value of H in per unit.

T_w = is the water starting time.

\bar{P}_m = mechanical power output in per unit.

\bar{U}_{NL} = no load water velocity in per unit.

The above equation gives the per unit value of the turbine power output on a base equal to the turbine Mega-Watt (MW) rating. Solution of the machine swing equation requires turbine mechanical torque on a base equal to either the generator Mega-Volt Ampere (MVA) rating or a common MVA base. Hence,

$$T_m = \left(\frac{\omega_0}{\omega}\right) \bar{P}_m \left(\frac{P_r}{MVA_{base}}\right) = \frac{1}{\bar{\omega}} (\bar{U} - \bar{U}_{NL}) \bar{H} \bar{P}_r \quad \dots (18)$$

Where

ω_0 = no-load speed in (revolution per minute), ω = actual speed in (revolution per minute), $\bar{\omega}$ = per unit speed.

MVA_{base} = base MVA on which turbine torque is to be made per unit

$$\bar{P}_r = \text{per unit turbine rating} = \frac{\text{turbine MW rating}}{MVA_{base}}$$

In the above equations, \bar{G} is the ideal gate opening based on the change from no load to full load being equal to 1 per unit. This is related to the real gate opening. The ideal gate opening is related to real gate opening as follows.

$$\bar{G} = A_t \bar{g} \quad \dots(19)$$

Where A_t is the turbine gain given by

$$A_t = \frac{1}{\bar{g}_{FL} - \bar{g}_{NL}} \quad \dots(20)$$

\bar{g} = real gate opening.

\bar{g}_{FL} = full load gate opening.

\bar{g}_{NL} = no load gate opening.

Figure (4) represents the Hydraulic turbine block diagram.

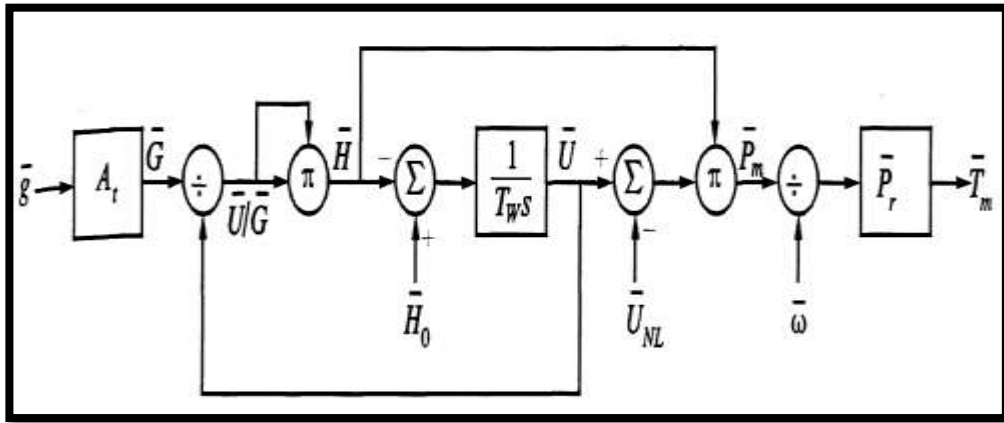


Figure (4) Hydraulic turbine block diagram.

HYDRAULIC GOVERNOR

The main function of the turbine-governing system is to regulate the turbine-generator speed and hence the frequency and the active power in response to load variation. The speed governor normally actuates the governor-controlled gates that regulate the water input to the turbine through the speed control mechanism [5].

The speed control function involves feeding back speed error to control the gate position. In order to ensure satisfactory and stable parallel operation of multiple units, the speed governor is provided with permanent droop (R_p) characteristic [11].

A very high force is required in governing systems for hydraulic turbines to move the control gate as it must overcome both high water pressure and high friction forces. To provide the necessary force to move the gate two servomotors are used as shown in the functional diagram in Figure (5). The speed regulator acts through a system of levers on the pilot valve which controls the flow of hydraulic fluid into the pilot servomotor. The pilot servomotor then acts on the relay valve of

the very high-power main servomotor which controls the gate position. Negative feedback of the position of both the servomotors is necessary to achieve the required movement.

The main servomotor is modeled with two limiters. The first limiter limits the gate position between fully open and fully closed, while the second, the rate limiter, limits the rate at which the gate can be moved. This is necessary because, if the gate is closed too rapidly, the resulting high pressure could damage the penstock [10].

Hydro turbines have a peculiar response due to water inertia: a change in gate position produces an initial turbine power change which is opposite to that sought. For stable control performance, a large transient (temporary) droop with a long resetting time is therefore required. This is accomplished by the provision of a rate feedback or transient gain reduction compensation. The rate feedback retards or limits the gate movement until the water flow and power output have time to catch up. The result is a governor which exhibits a high droop (low gain) for fast speed deviations, and the normal low droop (high gain) in the steady state [11].

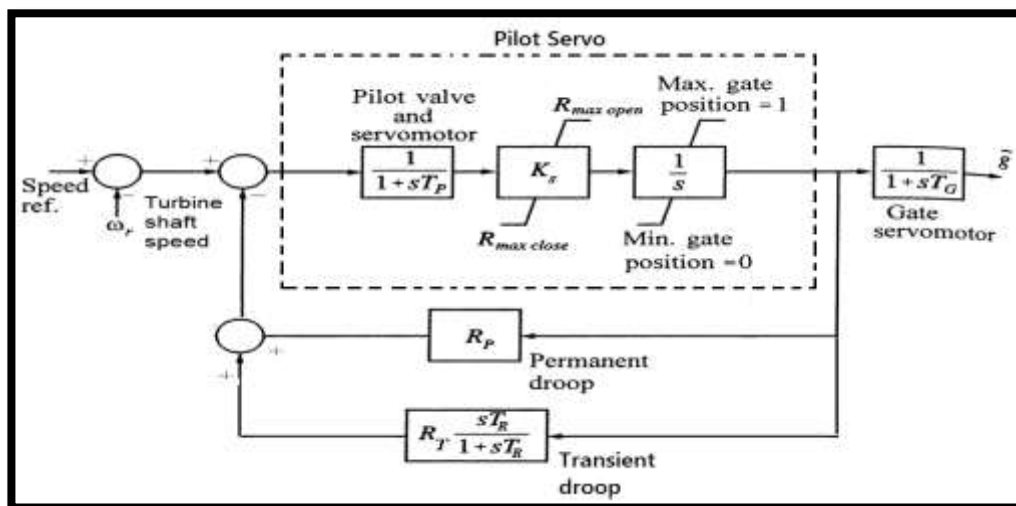


Figure (5) Model of Governors for Hydraulic Turbines [11].

T_G = main servomotor time constant, T_p = pilot servomotor time constant, R_p = permanent droop, $R_{max\ open}$ = maximum gate opening rate, $R_{max\ close}$ = maximum gate closing rate, R_T = temporary droop, T_R = reset time.

PID GOVERNOR

The Electro-Hydraulic governor uses the three-term PID-controller to perform the low-power functions. The proportional term produces a control action proportional to the size of the error input, and an immediate response to an error level input. The proportional term response has a significant influence on the stability of the governed system. The integral term produces a control action that accumulates at a rate proportional to the size of the error input. The integral term also trims out the error input to the governor controller to determine the steady-state accuracy of the governed system. The derivative term produces a control

action that is proportional to the rate of change of the error input [5]. However, the use of a high derivative gain or transient gain increase will result in excessive oscillations and possibly instability when the generating unit is strongly connected to an interconnected system. Therefore, the derivative gain is usually set to zero; without the derivative action, the transfer function of a PID (now PI) governor is equivalent to that of the mechanical-hydraulic governor. The proportional and integral gains may be selected to result in the desired temporary droop and reset time [11]. The PID governor is shown in Figure (6).

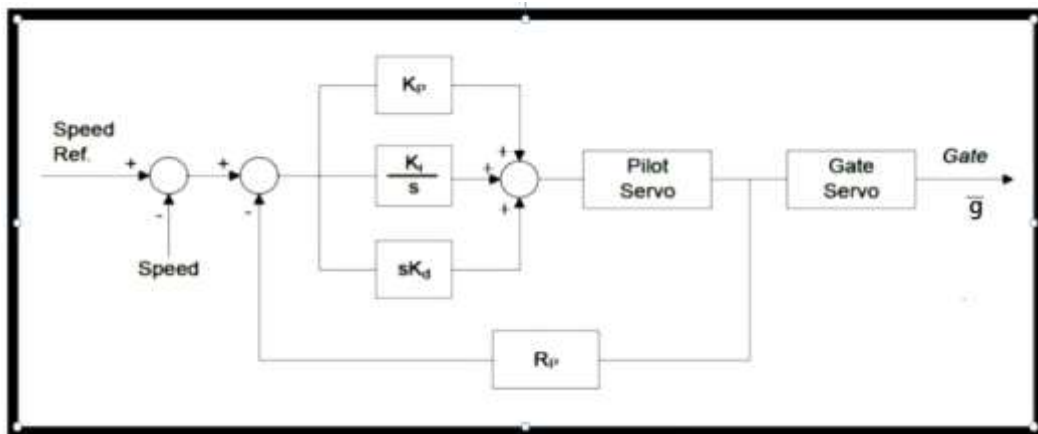


Figure (6) PID governor.

OVERVIEW OF PARTICLE SWARM OPTIMIZATION

Particle swarm optimization, first developed by Kennedy and Eberhart, is one of the modern heuristic algorithms. It was inspired by the social behavior of bird and fish schooling, and has been found to be robust in solving continuous nonlinear optimization problems. This algorithm is based on the following scenario: a group of birds are randomly searching food in an area and there is only one piece of food. All birds are unaware where the food is, but they do know how far the food is at each time instant. The best and most effective strategy to find the food would be to follow the bird which is nearest to the food. Based on such scenario, the PSO algorithm is used to solve the optimization problem. In PSO, each single solution is a “bird” in the search space; this is referred to as a “particle”. The swarm is modeled as particles in a multidimensional space, which have positions and velocities. These particles have two essential capabilities: their memory of their own best position and knowledge of the global best. Members of a swarm communicate good positions to each other and adjust their own position and velocity based on good positions according to equation (21 & 22).

$$v(k+1)_{i,j} = w.v(k)_{i,j} + c_1r_1(gbest - x(k)_{i,j}) + c_2r_2(pbest_j - x(k)_{i,j}) \quad \dots(21)$$

$$x(k+1)_{i,j} = x(k)_{i,j} + v(k)_{i,j} \quad \dots(22)$$

Where $v_{i,j}$: Velocity of particle i and dimension j, $x_{i,j}$: Position of particle i and dimension j, c_1, c_2 : Acceleration constants, w: Inertia weight factor, r_1, r_2 : Random numbers between 0 and 1, pbest: Best position of a specific particle,

gbest: nBest particle of the group [12]. The flow chart of Figure (7) shows the PSO algorithm.

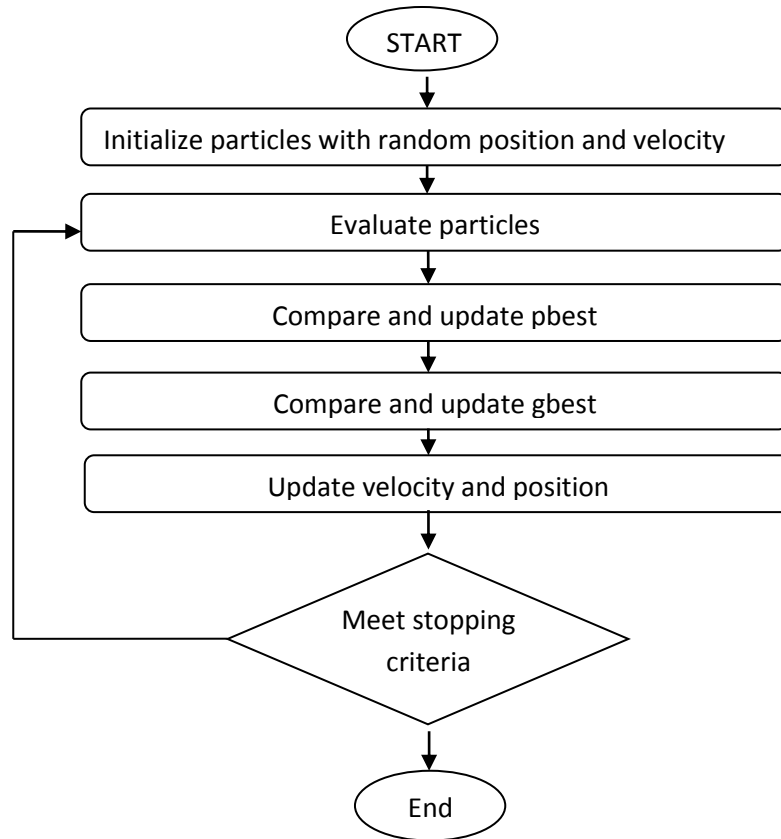


Figure (7) Flow chart of PSO algorithm.

PERFORMANCE INDICES

Performance index is defined as a quantitative measure to depict the system performance of the designed PID controller. Using this technique an ‘optimum system’ can often be designed and a set of PID parameters in the system can be adjusted to meet the required specification. For a PID- controlled system, there are often four indices to depict the system performance [13]:

$$\text{Integral Square Error (ISE)} = \int_0^{\infty} e^2(t). dt \quad \dots (23)$$

$$\text{Integral Absolute Error (IAE)} = \int_0^{\infty} |e(t)|. dt \quad \dots(24)$$

$$\text{Integral Time Absolute Error (ITAE)} = \int_0^{\infty} t. |e(t)|. dt \quad \dots(25)$$

$$\text{Integral Time Square Error (ITSE)} = \int_0^{\infty} t. e^2(t). dt \quad \dots(26)$$

Therefore, for the PSO-based PID tuning, these performance indices (Equations 23-26) will be used as the objective functions. In other words, the objective in the PSO-based optimization is to seek a set of PID parameters such that the feedback control system has minimum performance index.

FUZZY LOGIC

Fuzzy logic has received a lot of attention in the recent years because of its usefulness in reducing the model's complexity in the problem solution. It employs linguistic terms that deal with the causal relationship between input and output constraints. This logic was developed based on Lotfi Zadeh's 1960s fuzzy set theory [14]. The fuzzy controller is composed of the following four elements:

- 1) A rule-base (a set of If-Then rules), which contains a fuzzy logic quantification of the expert's linguistic description of how to achieve good control.
- 2) An inference mechanism (also called an "inference engine" or "fuzzy inference" module), which emulates the expert's decision making in interpreting and applying knowledge about how best to control the plant.
- 3) A fuzzification interface, which converts controller inputs into information that the inference mechanism can easily use to activate and apply rules.
- 4) A defuzzification interface, which converts the conclusions of the inference mechanism into actual inputs for the process.

FUZZY PID CONTROLLER

The design of a fuzzy-PID controller can be achieved in different ways. One way is to build a fuzzy controller with three inputs: the error (proportional action), the delta error (derivative action) and the sum of the error (integral action). The inconvenience for such a controller is that the number of rules will grow making the tuning task very difficult. A more efficient solution is to divide the controller in two controllers, one that is the PD equivalent and another one that provides the integral action. It will reduce the number of rules [15].

SIMULATION AND RESULTS

In this work, a salient pole synchronous generator of parameters shown in appendix B is used. Four different loads applied to the generator to test the controller behavior for different loading conditions, and to show the ability of the governor to control the SG frequency for a wide range of loading. The generator loading conditions are:

- 1- The SG loaded at (0.2 P.U) of its rated current as a light load.
- 2- After (20 second) the SG loaded at (0.5 P.U) of its rated current as medium load.
- 3- After (30 second) the SG loaded at full load (1 P.U).
- 4- After (40 second) the SG loaded at (1.1 P.U) of its rated current as over loading conditions.

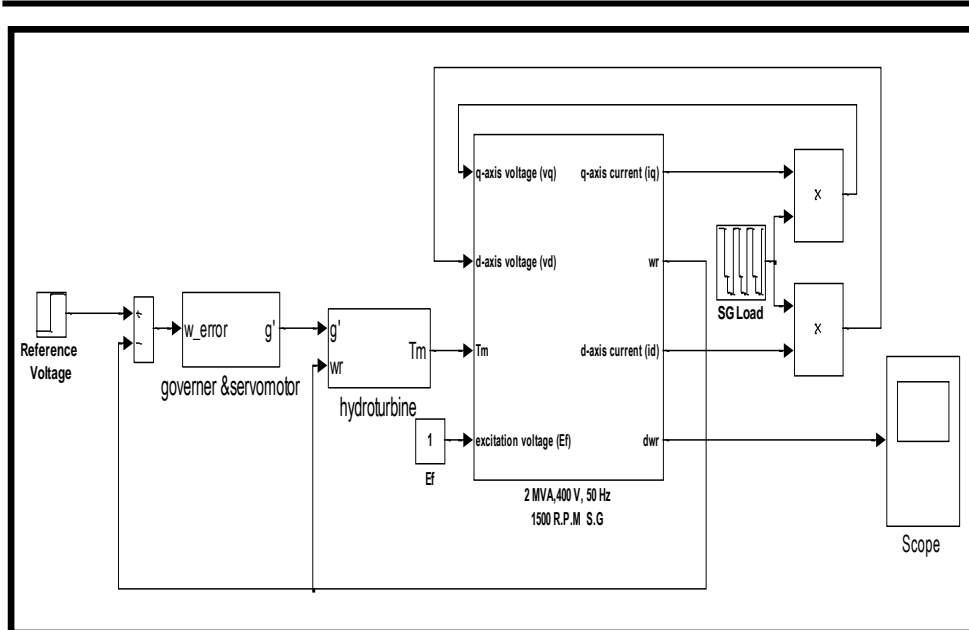


Figure (8) Simulink program of SG with turbine-governor model.

The simulink of hydraulic turbine block & governor block with PI-controller are shown in Figure (9) & Figure (10) respectively.

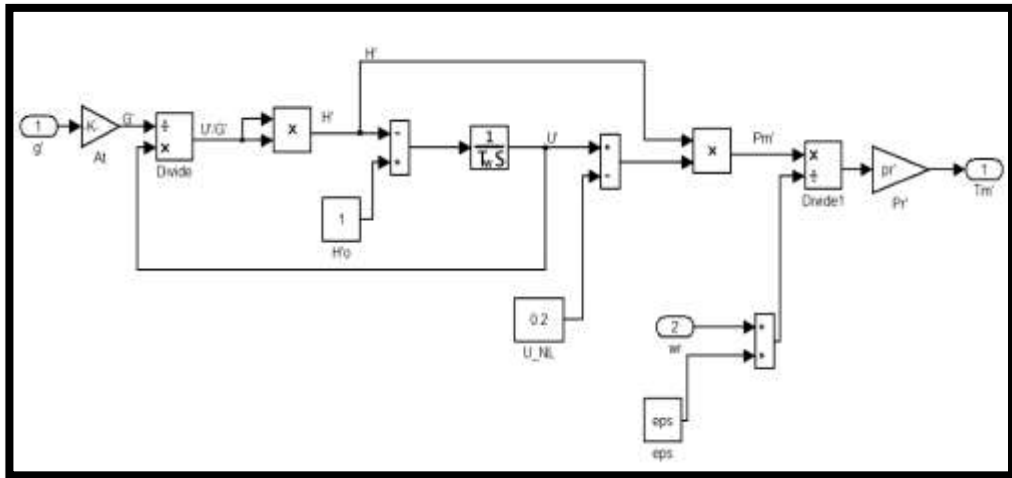


Figure (9) Simulink program of Hydraulic turbine block.

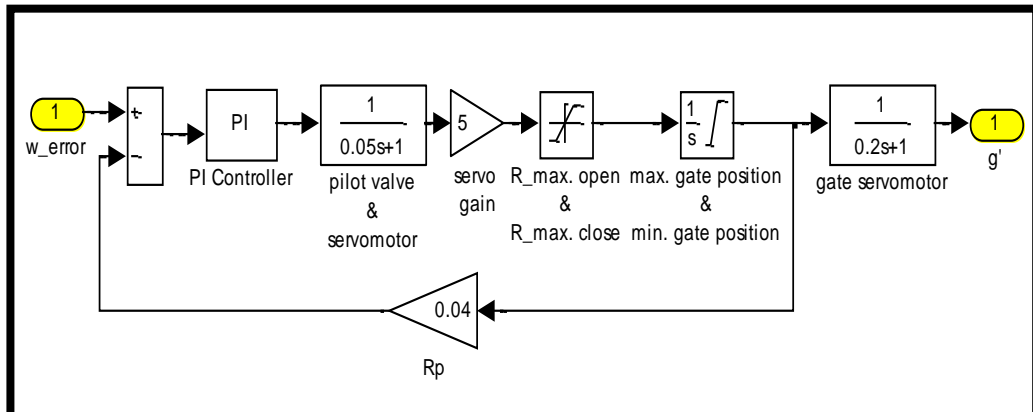


Figure (10) Simulink program of governor block.

The Hydraulic turbine and governor parameters which are used in the simulation are expressed in PU system as shown in Appendix C and Appendix D respectively.

Speed-Governor with PI-controller

The gains of PI controller tuned by trial and error method are $K_p = 4$ and $K_i = 9$.

The frequency deviation step responses of the SG with PI-controller tuned by trial and error method for different loads applied individually are shown in Figure (11).

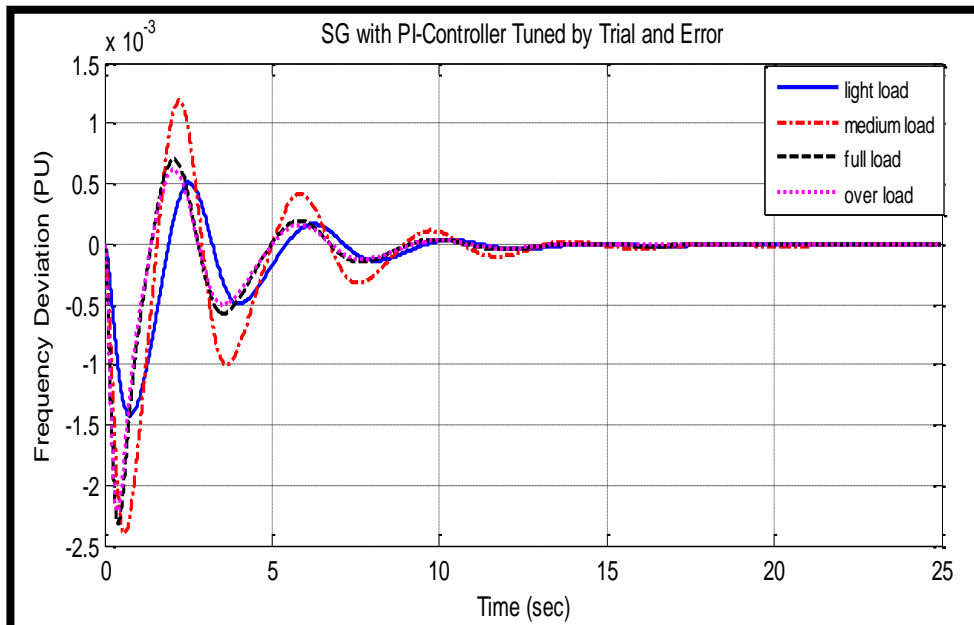


Figure (11) Frequency deviation step responses of the SG with PI controller tuned by trial and error method for different loads.

The frequency deviation step responses of PI-controller with gains tuned by trial and error method have a very large settling time and oscillation with large

overshoot and undershoot so it is important to use PSO tuning method to improve the system performance.

The PSO tuning method in this work depends on ITAE performance index. The parameter values of the PSO algorithm that achieved better solution are listed in Table (1).

Table (1) The parameters of PSO algorithm for tuning gains.

Swarm size (Number of birds)	30
Number of iterations	30
Cognitive coefficient (C_1)	2
Social coefficient (C_2)	2
Inertia weight (w)	0.5

The tuning process done while the SG was loaded at the four different loads (From light load to over load) at different time, this process enables the PSO algorithm to choose the optimal value of controller gains even for any value of load.

This tuning method make the controller robust for different load apply to the SG. The optimal gains of PI-controller tuned by PSO method are $K_p = 13.3081$ and $K_i = 9.1836$.

The frequency deviation step responses of the SG with PI-controller tuned by PSO for are shown in Figure (12).

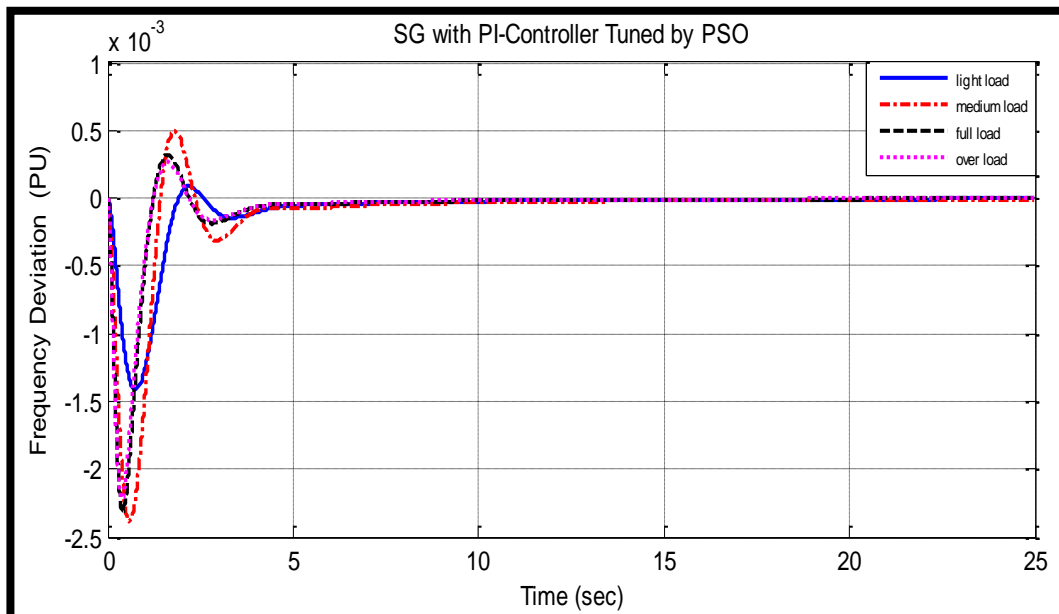


Figure (12) Frequency deviation step responses of the SG with PI- controller tuned by PSO for different loads.

Figure (13) shows step response of SG with PI controller which gains tuned by trial and error and PSO for different loads applying during operation as stated previously.

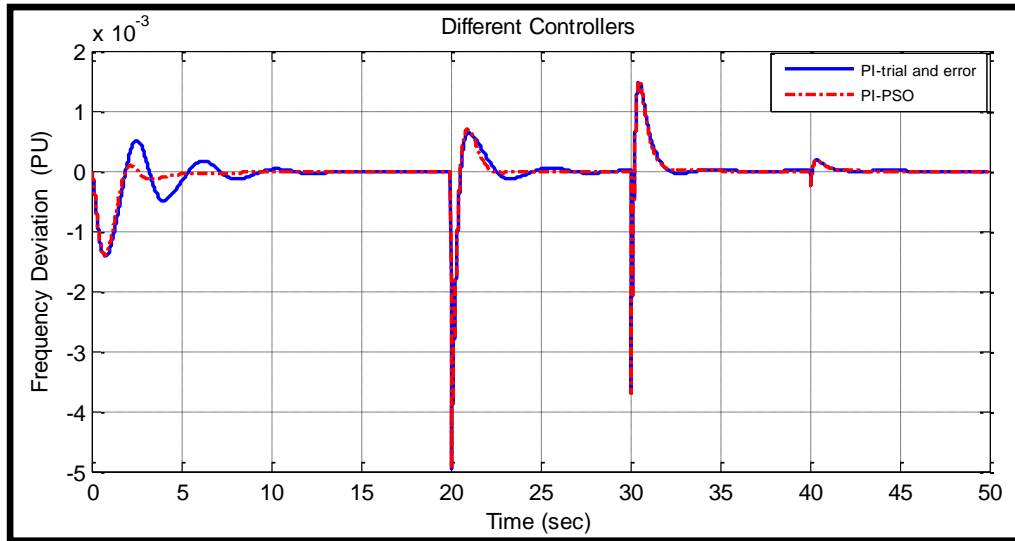


Figure (13) Frequency deviation step response of the SG with PI-controller tuned by trial and error method and by PSO with load change from light to over load.

The results of PI-controller tuned by PSO shows the superiority in performance of this controller versus the PI-controller tuned by classical trial and error method. The PI-controller tuned by PSO reduces the overshoot and settling time while the undershoot remain approximately the same.

Simulation of Speed-Governor Model with Fuzzy PD+I-Controller:

A proposed Fuzzy PD+I controller with gains and MFs parameters optimized by PSO technique is used in order to enhance the performance of controller. Figure (14) illustrates the simulation model of governor with Fuzzy PD+I-controller.

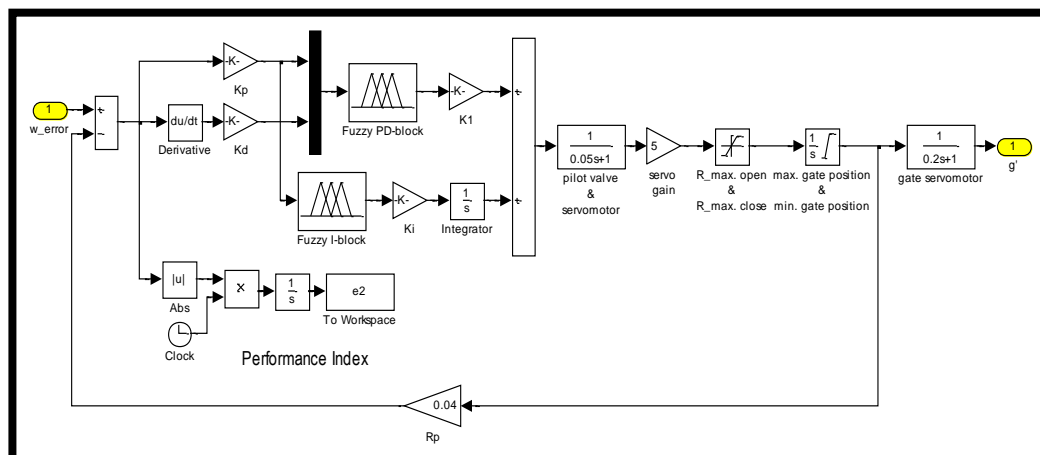


Figure (14) Simulink program of governor with Fuzzy PD+I- controller.

PD and I-blocks rules are shown in Table (2) and Table (3) respectively.

Table (2) PD- block rules

input	output
N	N
Z	Z
P	P

Table (3) I- block rules.

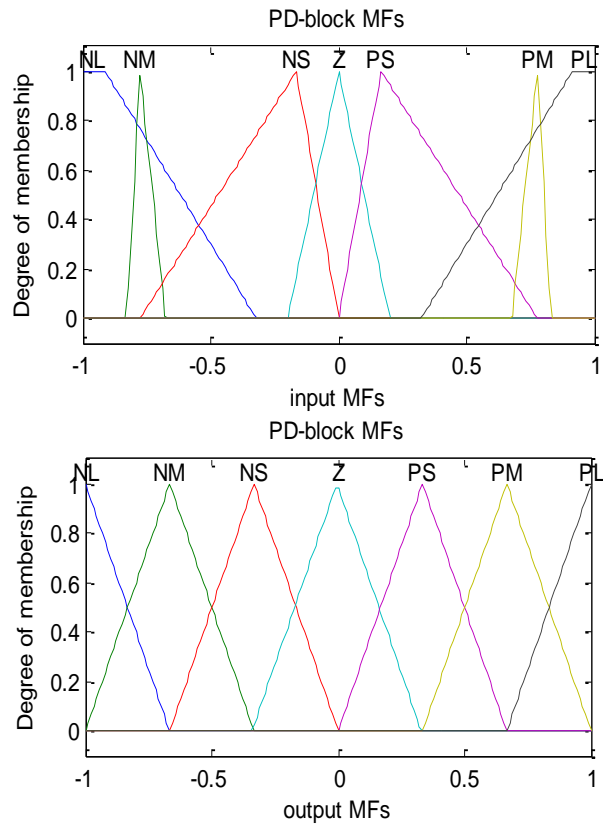
e Δe	NL	NM	NS	Z	PS	PM	PL
NL	NL	NL	NL	NL	NM	NS	Z
NM	NL	NL	NM	NM	NS	Z	PS
NS	NL	NM	NM	NS	Z	PS	PM
Z	NM	NM	NM	Z	PS	PM	PM
PS	NM	NS	Z	PS	PM	PM	PL
PM	NS	Z	NS	PM	PM	PL	PL
PL	Z	PS	PM	PL	PL	PL	PL

Parameters of PSO algorithm used for tuning gains are shown in Table (4).

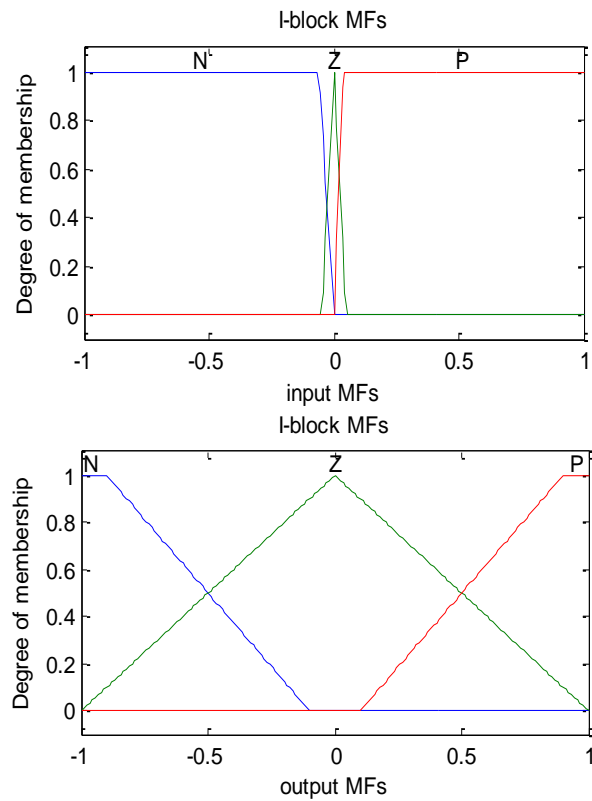
Table (4) Parameters of PSO algorithm for tuning input MFs and gains of Fuzzy PD+I controller.

	For MFs tuning	For gains tuning
Swarm size (Number of birds)	10	10
Number of iterations	10	20
Cognitive coefficient (C_1)	1.2	2.05
Social coefficient (C_2)	1.2	2.05
Inertia weight (w)	0.9	0.4

Figure (15) and Figure (16) shows the input/output tuned input MFs of PD-block and I-block respectively.



(a) Input (1) & (2) MFs (b) Output MFs
Figure (15) Input/output MFs of PD-block after tuning process



(a) Input (1) MFs (b) Output MFs
Figure (16) Input/output MFs of I-block after tuning process.

The frequency deviation step responses of the SG with Fuzzy PD+I-controller for different loads applied individually are shown in Figure (17).

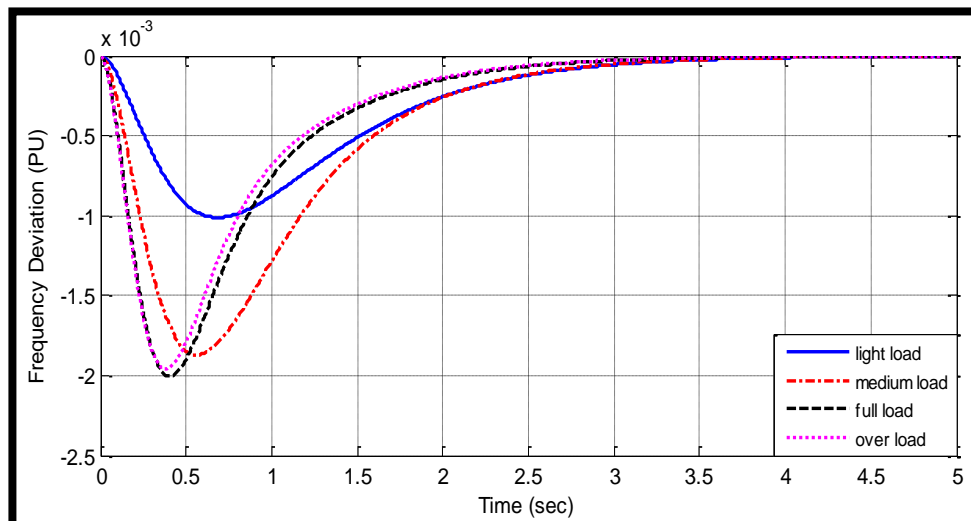


Figure (17) Frequency deviation step responses of SG with Fuzzy PD+I controller for different loads.

Figures (18) and (19) show the comparison in frequency deviation step response of SG for the four controllers with four different loads.

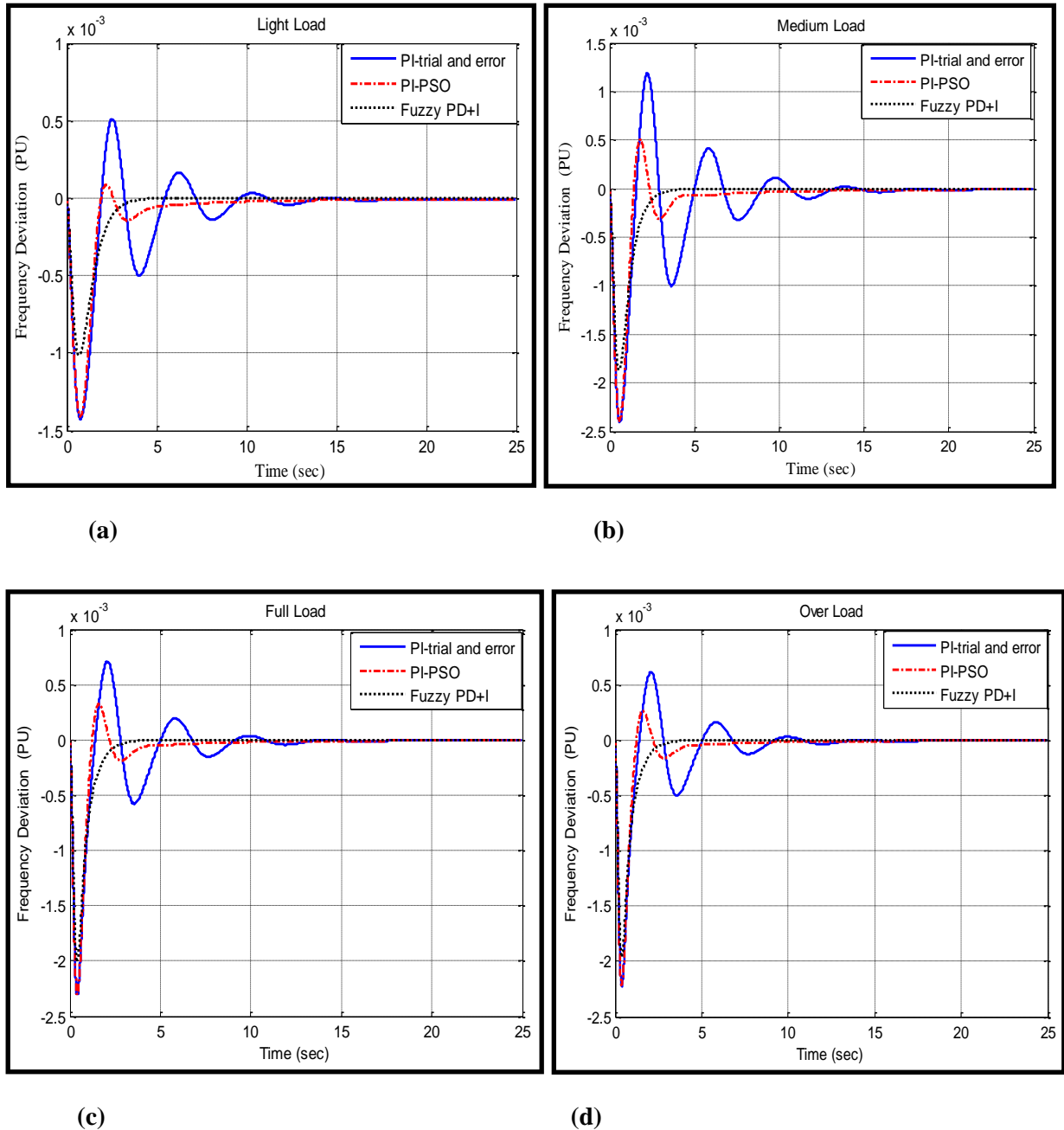


Figure (18) Frequency deviation step responses of SG with different loads. (a) With light load. (b) With medium load. (c) With full load. (d) With over load.

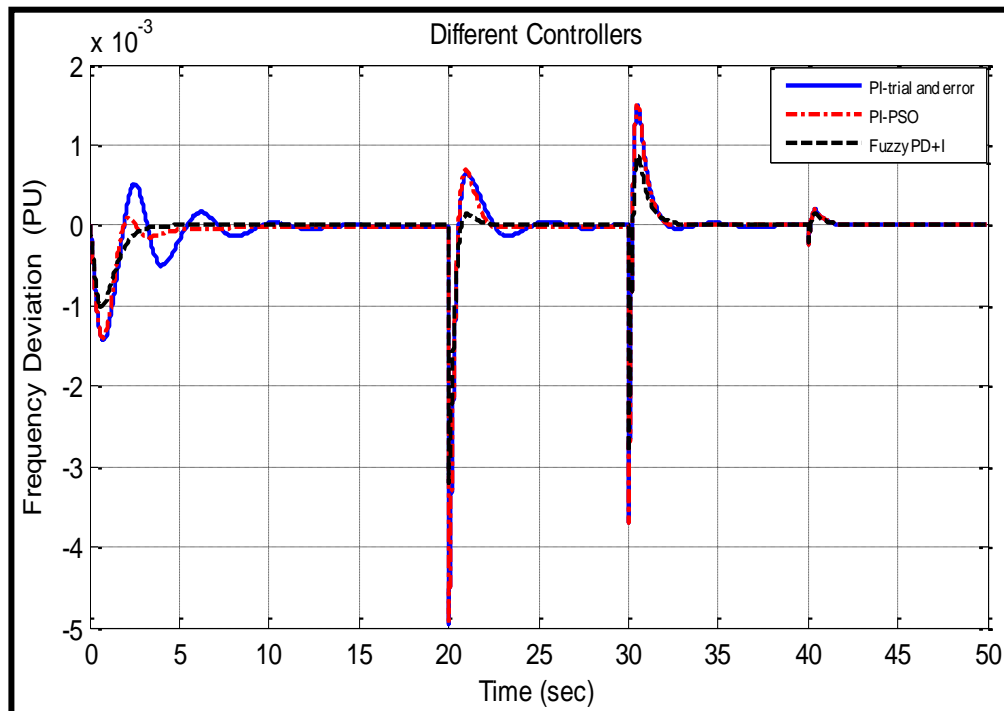


Figure (19) Comparison in frequency deviation step responses of SG for load changes from light to over load.

CONCLUSIONS

The PI controller is normally used in the industry due to its simple structure, and the ability to apply for a wide range of situations. The selection of the controller gains are difficult and time consuming. To overcome this difficulty the PSO is used to find optimal gains. PSO tuning technique consumes less time and has fast convergence than trial and error method. The PSO tuning method makes the controller superior than controller with trial and error tuning method.

The use of the PI controller tuned by PSO technique can improve the performance of speed-governor compared with classical PI controller. For light load, undershoot reduces by 0.86%, overshoot by 83% and settling time at error $\leq |10^{-5}|$ by 0.1%. For medium load, undershoot reduces by 0.44%, overshoot by 58% and settling time at error $\leq |10^{-5}|$ by 3.3%. For full load undershoot reduce by 0.06%, overshoot by 55% and settling time by 10.5%. For over load undershoot reduce by 0.04%, overshoot by 56.6% and settling time at error $\leq |10^{-5}|$ by 16.4%.

The Fuzzy PD+I controller has the difficulties in selecting the gains and parameters of MFs of the Fuzzy PD+I controller which can be overcome by using PSO technique. The use of the PSO technique can improve the performance of speed-governor with Fuzzy PD+I controller compared with PI-PSO controller. For light load undershoot reduce by 28.4%, overshoot by 100% and settling time at

error $\leq |10^{-5}|$ by 76%. For medium load undershoot reduce by 21.8%, overshoot by 100% and settling time at error $\leq |10^{-5}|$ by 82%. For full load undershoot reduce by 13.2%, overshoot by 100% and settling time by 76.3%. For over load undershoot reduce by 12%, overshoot by 100% and settling time at error $\leq |10^{-5}|$ by 74.7%.

REFERENCES

- [1]. Cirstea, M. N. A. Dinu, J.G. Khor, M.M. Cormick, "Neural and Fuzzy Logic Control [] of Drives and Power Systems", Linacre House, Jordan Hill, 2002.
- [2]. Soundarrajan, A. S. Sumathi, C. Sundar, "Particle Swarm Optimization Based LFC [] and AVR of Autonomous Power Generating System", IAENG International Journal [] of Computer Science, Vol.37, Issue 1, 2010.
- [3]. Saadat, H. "Power System Analysis", McGraw-Hill Inc., 1999.
- [4] I. Boldea, "Synchronous Generators", 1st Edition by Taylor & Francis Group, LLC, [] 2006.
- [5]. Lucero, L. A. "Hydro Turbine and Governor Modelling", Norwegian University of [] Science and Technology Dept. of Electric Power Engineering, M.Sc. Thesis, [] 2010.
- [6]. Altas, I. H. and J. Neyens, "A Fuzzy Logic Load-Frequency Controller for Power [] Systems", International Symposium on Mathematical Methods in Engineering, [] MME-06, Cankaya University\Ankara, Turkey, April 27-29, 2006.
- [7]. Park, R. H. "Two-Reaction Theory of Synchronous Machines", NAPS University [] of Waterloo, Canada, October 23-24, 2000.
- [8]. Sharma, D. "Investigation on Transient Performance of Superconducting Generator [] with Governor Control and Stabilizer", Thapar University, Patiala, Electrical and [] Instrumentation Engineering Department, M.Sc. Thesis, July, 2009.
- [9]. Chee-Mun Ong, "Dynamic Simulation of Electrical Machinery Using Matlab [] Simulink", 3rd Edition published by Prentice Hall PTR, 1998.
- [10]. Machowski, J. J. W. Bialek, J. R. Bumby, "Power System Dynamics Stability and [] Control", 2nd Edition, John Wiley & Sons, Ltd, 2008.
- [11]. Kundur, P. "Power System Stability and Control", McGraw-Hill, 1994.
- [12]. Yan, Y. W. A. Klop, M. Molenaar, P. Nijdam, "Tuning a PID controller: Particle [] Swarm Optimization versus Genetic Algorithms", February, 2010.
- [13]. Solihin, M. I. L. F. Tack and M. L. Kean, "Tuning of PID Controller Using Particle [] Swarm Optimization (PSO)", Proceeding of the International Conference on [] Advanced Science, Engineering and Information Technology, Malaysia, 14-15 [] January 2011.
- [14]. Angelina Borges de Rezende Costa, Ana Claudia Marques do Valle, Adélio José de [] Moraes and Haroldo R. de Azevedo, "A Simple Fuzzy Excitation Control System [] (AVR) In Power System Stability Analysis".
- [15]. [] Espinosa, J. J. Vandewalle and V. Wertz, "Fuzzy Logic, Identification and [] Predictive Control", Springer-Verlag London Limited, 2005.

Appendix A

The block diagrams of q-circuit, d-circuit and rotor circuit shown in Figure (2) of section 2

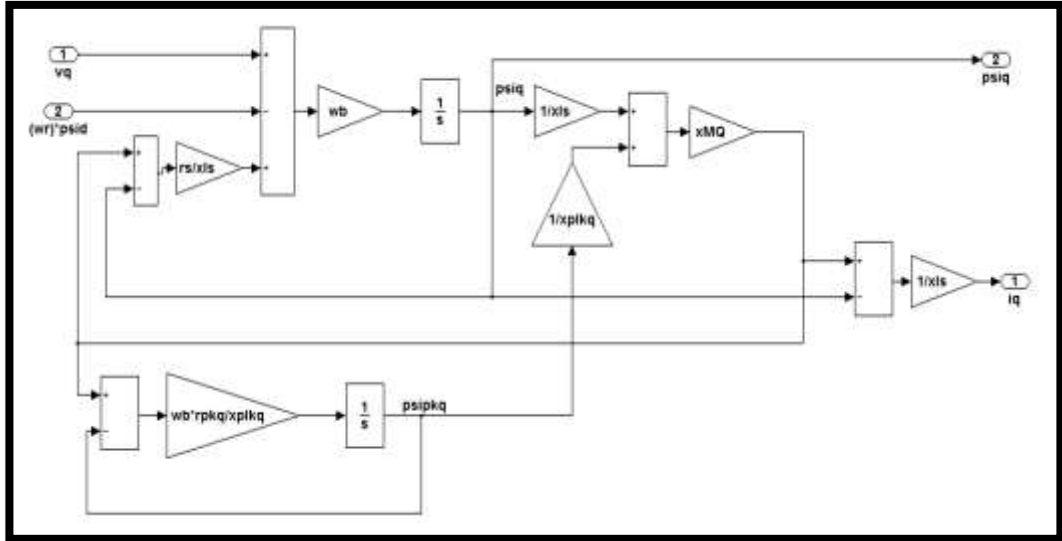


Figure (A-1) q- circuit of Figure (2).

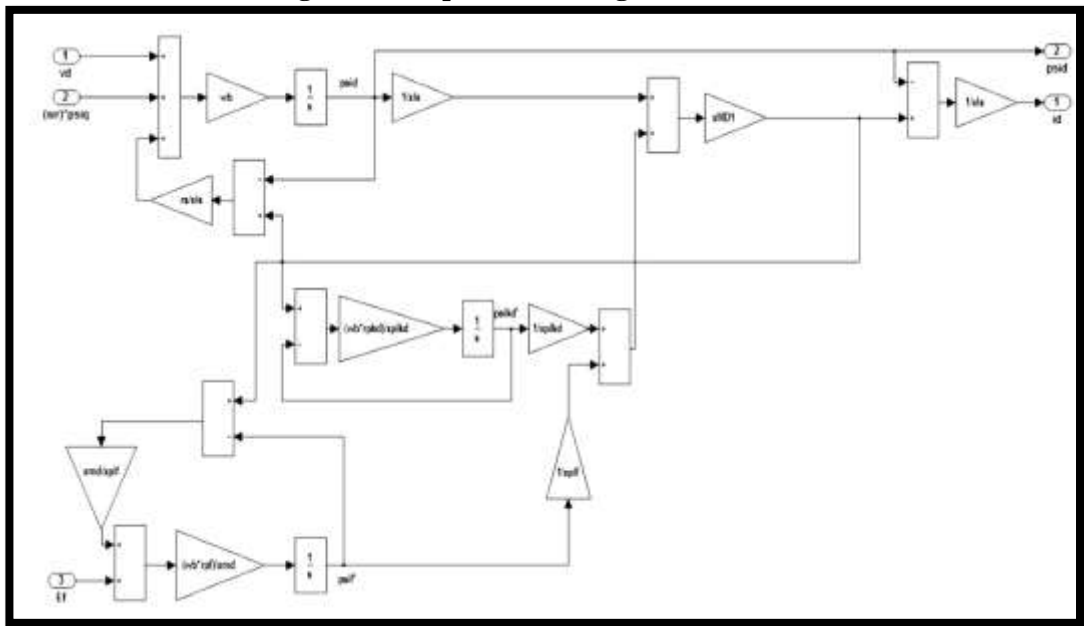


Figure (A-2) d- circuit of Figure (2) .

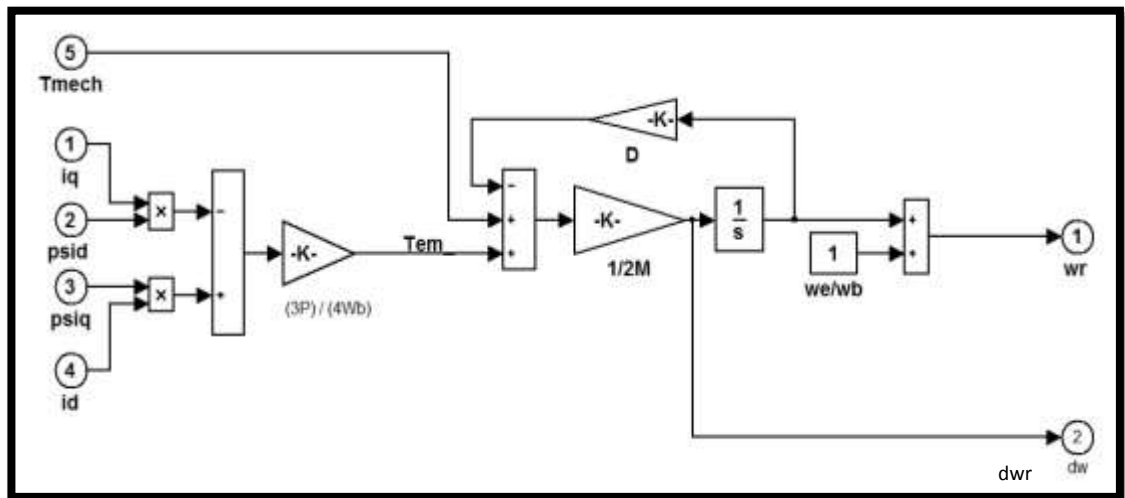


Figure (A-3) Rotor block of Figure (2).

Appendix B

The table below shows the (2 MVA) SG parameters taken from the Matlab simulink tool box which used in our simulation model.

Table (A-1) The salient pole SG parameters value from MATLAB/Toolbox.

Rated Power	KVA	2000
Rated voltage	V(L-L)	400
Rated frequency	HZ	50
stator resistance(rs)	pu	0.0095
stator leakage inductance (Lls)	pu	0.05
mutual inductance of d-axis(Lmd)	pu	2.06
mutual inductance of q-axis(Lmq)	pu	1.51
field resistance on d-axis(rf')	pu	.001971
field leakage inductance on d-axis(Llf')	pu	0.3418
damper resistance n d-axis(rkd')	pu	0.2013
damper leakage inductance on d-axis(Llkd')	pu	2.139
damper resistance on q-axis(rkq')	pu	0.02682
damper leakage inductance on q-axis(Llkq')	pu	0.2044
Inertia coefficient (H)	pu	0.3072

Appendix C

The Hydraulic turbine parameters which used in the simulation are expressed in PU system and shown in Table (B-1).

Table (B-1) Hydraulic-turbine parameters [11].

\bar{g}_{FL}	0.96 PU
\bar{g}_{NL}	0.16 PU
At	1.25 PU
Tw	Sec 1
Pr	1 PU
H' ₀	1 PU
U _{NL}	0.2 PU

Appendix D

The Hydraulic governor parameters which used in the simulation are expressed in PU system and shown in Table (C-1).

Table (C-1) Hydraulic-governor parameters [11].

T _p	0.05 Sec
K _s	5 PU
T _G	0.2Sec
R _p	0.04 PU
Maximum gate position limit	1 PU
Minimum gate position limit	0 PU
R _{max} open	0.16 PU/Sec.
R _{max} close	0.16 PU/Sec.